A Novel Method to Evaluate the Neurocompatibility of Dental Implants

Mohammad Ali Saghiri, BSc, MSc, PhD[1]/Mahmood Ghasemi, DDS, MS[2]/
Amir Reza Moayer, DDS, MS[3]/Nader Sheibani, BSc, MSc, PhD[4]/
Franklin Garcia-Godoy, DDS, MS, PhD[5]/Armen Asatourian, DDS[6]/Hoori Aslroosta, DDS, MS[7]

Purpose: *To evaluate the neurocompatibility of different types of dental implant surface treatments using the P19 neural cell line.* ***Materials and Methods:*** *P19 cells were plated and supplemented with retinoic acid to grow as aggregates for 4 days. Twenty dental implants were selected from four different implant systems with five different surface treatments. The implants were divided into four groups (n = 5), placed inside medical rings, and fixed by injection of warm gutta-percha using a thermoplastic injection technique. Implant molds were placed inside graded culture dishes, and culture medium containing P19 neural cells were plated on the dishes for 4 days. After 24 hours, the surfaces of the implant molds were covered with self-curing resin to make a replica of each mold surface. Replicas were assessed under a scanning electron microscope, and the number of cells and the total cells covering the areas were evaluated. Data were analyzed by a post hoc Tukey test.* ***Results:*** *There were significant differences in P19 cell counts between all modified and electropolished surfaces. The highest P19 cell counts were shown on OsseoSpeed and Laser-Lok surfaces. The lowest counts were shown on the Nanotite surface at the collar. OsseoSpeed and Laser-Lok surfaces showed higher counts at the collar than on the body; the opposite was seen for SLActive and Nanotite surfaces. Cell-covered areas on Laser-Lok surfaces showed significantly higher values than the resorbable blasted media (RBM)–treated surfaces, while it was not significantly different from the OsseoSpeed surface of collar regions. SLActive collar regions showed larger cell-covered areas than the SLActive body surfaces, but this was not significant.* ***Conclusion:*** *All test surface treatments in this study showed better neurocompatibility than control group surfaces. The Laser-Lok, RBM, and OsseoSpeed surfaces were superior to the Nanotite and SLActive surfaces in terms of neurocompatibility.* Int J Oral Maxillofac Implants 2014;29:41–50. doi: 10.11607/jomi.3188

Key words: *dental implants, neurocompatibility, P19 cell line, titanium*

Since the introduction of osseointegration and root-form dental implants, many attempts have been made to develop more bone-to-implant contact. Numerous implant surface treatments, such as SLActive, OsseoSpeed, Laser-Lok, and Nanotite, have been used to improve implant surface microtopography and properties to accelerate osseous integration.[1] The biocompatibility of dental implants has been widely discussed in the literature.[2–7] In recent studies, some investigators have claimed that titanium dioxide (TiO_2) particles could induce inflammatory responses in lung tissues and even cytotoxicity in lung cells according to their micro- and nanoparticle size and surface chemistry. These particles can affect astrocytelike astrocytoma U87 cells in an irreversible way, depending on the concentration of these particles.[2–5] Hence, the metallic oxides such as TiO_2 used in dental and other implants may not be as benign as previously assumed on the basis of their biocompatibility.[6,7] Clearly, this area of nanotoxicity deserves further systematic investigation.

A few weeks after placement of dental implants, regeneration of intraosseous neural tissue occurs; this can lead to frequent contact between abundant nerve fibers and titanium dental implants throughout the bone.[8–10] Furthermore, one of the neglected components of

[1]Assistant Professor, Department of Dental Materials and Craniofacial Research Center, Dental School, Azad University (Tehran Branch), Tehran, Iran.
[2]Associate Professor and Head, Periodontics Department, Azad University (Tehran Branch), Tehran, Iran.
[3]Postgraduate Student, Periodontics Department, Azad University (Tehran Branch), Tehran, Iran.
[4]Professor, Department of Ophthalmology and Visual Sciences, University of Wisconsin School of Medicine and Public Health, Madison, Wisconsin, USA.
[5]Professor, Bioscience Research Center, College of Dentistry, University of Tennessee Health Science Center, Memphis, Tennessee, USA.
[6]Visiting Scientist, Kamal Asgar Research Center, Tehran, Iran.
[7]Private Practice, Tehran, Iran.

Correspondence to: Mohammad Ali Saghiri, Dental Materials Department, Azad University Tehran, P.O. Box 14665-1445, Tehran, Iran. Email: saghiri@gmail.com

©2014 by Quintessence Publishing Co Inc.

© 2014 BY QUINTESSENCE PUBLISHING CO, INC. PRINTING OF THIS DOCUMENT IS RESTRICTED TO PERSONAL USE ONLY.
NO PART MAY BE REPRODUCED OR TRANSMITTED IN ANY FORM WITHOUT WRITTEN PERMISSION FROM THE PUBLISHER.

tissue regeneration is neural regeneration. Neural cells, because of their greater susceptibility to free radical–mediated injuries, metabolic insults, and environmental toxins in comparison with fibroblasts, may require more sensitive methods for the assessment of biocompatibility.[11,12] Experimental studies of previously introduced surface treatments on different species have shown that titanium implants probably cannot have neurotoxic effects.[9,13] However, some authors have noted that the adsorption of implant surfaces inside the body might lead to systemic neurotoxicity.[5] P19 stem cells are the major cell lines available that can be used to evaluate the neurotoxicity of different materials. Studies of Saghiri et al and Khorasani et al have shown the suitability and reliability of cultured P19 stem cell testing for the evaluation of neurocompatibility.[14,15]

Four root-form dental implant types with five different surface treatments were used in this experimental study. Biomet 3i, AstraTech, and Straumann ITI have all introduced implants with different roughnesses (on the micro and nano levels) and physicochemical properties that have been tested in other studies.[16] Biohorizons is another popular manufacturer that produces two different types of surface treatments—resorbable blast media (RBM) for the implant body and Laser-Lok for the collar surface—giving it a unique surface topography. Biomet 3i's Nanotite surface represents a new nanocoated structure. This implant is supplied with attached nanohydroxyapatite compounds, which might be of particular interest for biocompatibility. Although previous studies used disk-shaped alloys,[17] the present study used the final product because it is commercially available (like the other implants, to prevent any potential conflicts of interest) and to evaluate the effect of storage and packaging on the applicable product by a novel technique. Each implant was evaluated in its collar and apical areas. The ITI implant featured an electropolished SLActive surface, which was present on the collar, and was used as a control. The Biomet 3i implant and collar featured the Nanotite surface, Biohorizons featured the RBM surface, the Biohorizons collar had a Laser-Lok surface, and Astra featured the OsseoSpeed surface on its body and its microthreaded collar. The neural cell line and the methodology of screening are complex; however, previous studies have confirmed the practicality of using replica methods for screening P19 neural cell lines.[14]

Regarding the inconsistent findings in relation to neurocompatibility of dental implant surfaces, the tested null hypotheses were: (*1*) the different surface treatments (electropolished SLActive, OsseoSpeed, Laser-Lok, RBM, Nanotite) do not have any effect on neurocompatibility or neurotoxicity of dental implants; and (*2*) these tested surface treatments do not increase P19 neuronal cell attachment behaviors or the orientation of these cells on the dental implant surfaces to promote osseoperception in the surrounding bone.[10]

MATERIALS AND METHODS

Cell Culture

The research protocol was approved by the Research Ethics Committee of Kamal Asgar Research Center (protocol no. KARC/17C2011-47-05). This part of the study was similar to work carried out previously by Saghiri et al.[14] In brief, the P19 stem cells (Pasteur Inst) were cultured from frozen stock by thawing the cells rapidly at 37°C; the cells were cultured in a standard medium, consisting of α-minimum essential medium (Gibco BRL, Life Technologies) supplemented with 7.5% calf serum (Gibco BRL, Life Technologies) and 5% fetal serum (Gibco BRL, Life Technologies) and containing 100 U/mL penicillin-streptomycin. The cells were maintained in subconfluent conditions by subculturing every 48 hours into tissue culture–grade dishes (Nunc). Thereafter, the culture dishes were treated with trypsin (Gibco BRL, Life Technologies) to induce neural differentiation in P19 stem cells. The cells were plated at a density of 5×10^4 cells/mL in the medium, supplemented with 0.3 mL of retinoic acid (RA) (Sigma) into 100-mL bacteriologic-grade Petri dishes initially and grown as aggregates for 4 days. The medium was refreshed every 48 hours during this period.

Group Preparations

Twenty dental implants of four different implant systems with five surface treatment types were selected as follows, along with control groups:

1. 3i (Biomet 3i): Nanotite surface (diameter: 5.6 mm, length: 15 mm; IFOS5615)
2. Astra (Astra Tech): OsseoSpeed surface (diameter: 5.0S mm, length: 10 mm; 24653)
3. Biohorizons: RBM for the body surface and Laser-Lok for collar surface (diameter: 5.8 mm, length: 10.5 mm; TLX5810)
4. ITI (Institute Straumann): SLActive surface; electropolished portion at the collar used as a control (HJ, diameter: 4.1 mm; length: 10 mm, 033.0525)
5. Gutta-percha (Mani) as a negative control
6. Zinc oxide eugenol (Kemdent, Associated Dental Products Ltd) as a positive control

After the implants were opened under aseptic conditions, they were placed inside polyurethane medical rings (Gerenzu) with an inner diameter of 21 ± 1 mm, an outer diameter of 25 ± 1 mm, and a height of 5 ± 1 mm. The medical rings and the implants inside them were

© 2014 BY QUINTESSENCE PUBLISHING CO, INC. PRINTING OF THIS DOCUMENT IS RESTRICTED TO PERSONAL USE ONLY.
NO PART MAY BE REPRODUCED OR TRANSMITTED IN ANY FORM WITHOUT WRITTEN PERMISSION FROM THE PUBLISHER.



Fig 1a Astra Tech implant placed inside polyurethane medical ring.



Fig 1b Beta Obturation system.



Fig 1c Gutta-percha injection by using Beta Obturation system inside the medical ring containing the implant.



Fig 1d Mold of Astratech implant. Note the implant notch in the apical third, facing upward inside the mold.



Fig 1e Measurement of the polyurethane ring's outer diameter by a digital caliper.



Fig 1f A replica is made of the prepared implant mold by applying resin to the surface of the mold.

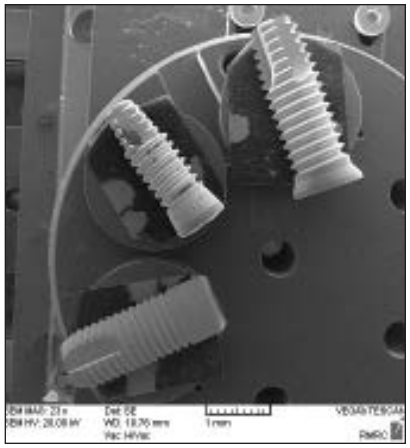

Fig 1g SEM image of three implants (*top to bottom*: Biomet 3i, Biohorizons, Astra Tech).

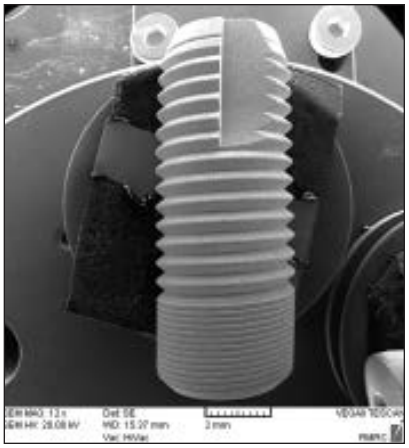

Fig 1h SEM image of Astra Tech implant.

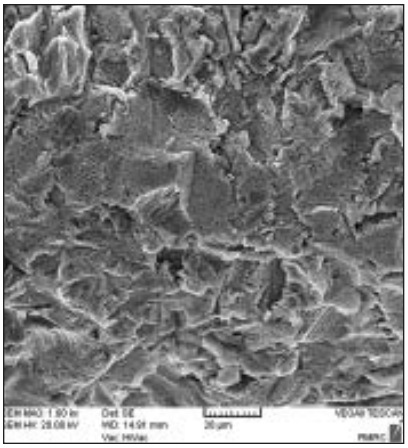

Fig 1i SEM image of the area of the Astra Tech implant notch in the apical third of the implant.

fixed on a microscopic slide measuring 4 × 3 inches (Ted Pella) and then were filled with gutta-percha using the Beta Obturation system (B&L Obturation, Biotech) so that molds of the implants could be used to easily transfer the implants to the culture medium. Finally, a suitable microcondenser was chosen to ensure proper fit of the samples into the plates of gutta-percha (Fig 1). Each specimen was placed in a separate vial and stored at 37°C. Pieces of gauze soaked in related media were used to cover all the specimens for 24 hours before cell culture testing. Wet pieces of gauze were replaced every 6 hours with fresh pieces to ensure a suitable environment within the vials. In the positive control group, the zinc oxide eugenol was prepared according to the manufacturer's instructions and placed inside a medical ring with the same diameter as those used for the dental implants; then the medical ring was filled with gutta-percha, similar to the experimental groups, to prepare zinc oxide–eugenol molds for further assessment. In the negative control group, the medical ring was filled with gutta-percha only, without any other material inside, to form a solid gutta-percha mold.

© 2014 BY QUINTESSENCE PUBLISHING CO, INC. PRINTING OF THIS DOCUMENT IS RESTRICTED TO PERSONAL USE ONLY.
NO PART MAY BE REPRODUCED OR TRANSMITTED IN ANY FORM WITHOUT WRITTEN PERMISSION FROM THE PUBLISHER.

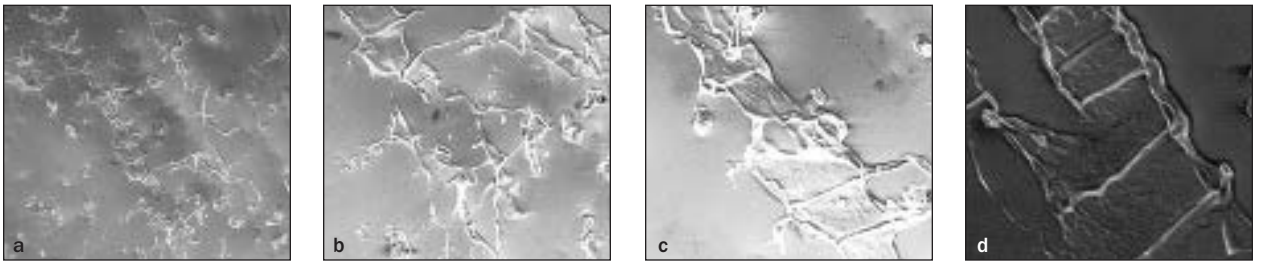

Figs 2a to 2d SEM images of the surface of replicas. (*a*) OsseoSpeed (Astra); (*b*) Nanotite (Biomet 3i); (*c*) Laser-Lok and RBM (Biohorizons); (*d*) SLActive (ITI).

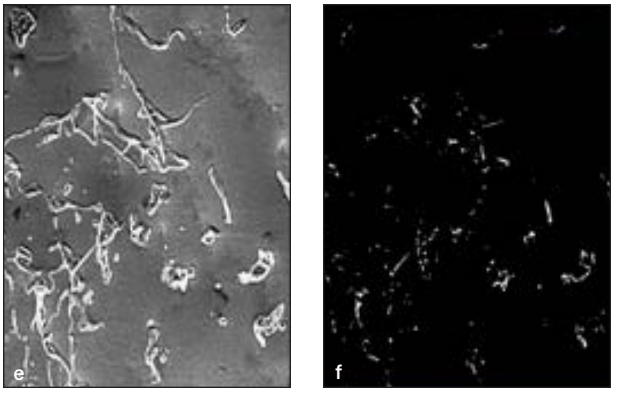

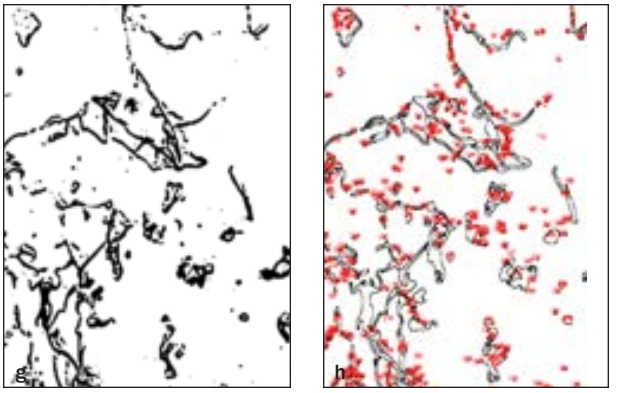

File Edit Font

Slice	Count	Total Area	Average Size	Area Fraction	Mear
OK.tif	346	2.456	0.007	9.2	0

i

Figs 2e to 2i The sequence of calculation of uniformity dispersion evaluated by Image J software. (*e*) Submicrograph (color dot mapped over the texture) (×1,000); (*f*) prepared scale for easy calculation and adjustment of brightness; (*g*) binarization; (*h*) adjustment of threshold for a better calculation; (*i*) analysis of the number of particles (islands) and the cell-covered surface.

Neurocompatibility Assay

After 4 days of RA treatment, the aggregates were plated onto the tissue culture-grade dishes containing implant molds and control groups in a medium without RA. Culturing continued for 4 days (molds were fixed into culture dishes with nickel-titanium needles to ensure that guttapercha was placed at the bottom of the culture plates). Immediately after the implant molds were retrieved from the tissue media, each mold was placed into a Petri dish and cooled to –70°C at a rate of 10°C/min (MDF-C8V1, Sanyo Electric Co). The Petri dishes were placed on a tray and stored in a freezer at –70°C for 24 hours.

Scanning Electron Microscopy

Immediately after the molds were retrieved from the freezer, a replica of each mold was prepared using resin (RepliSet-F1 50-mL System, Struers). The pre-polymer was mixed with the curing agent and placed immediately on each implant mold. After 20 minutes at room temperature, the replicas were cured. The peeled-off replicas were observed under a scanning electron microscope (SEM) (Leo 440i, Cambridge Instruments; and TESCAN) (Fig 2). Each replica was sputter-coated with gold and visualized under the SEM at 15 kV by a secondary detector.

A grading system was developed with respect to Image J software (U.S. National Institutes of Health). The following features were measured: (*1*) number of cells over the surface, and (*2*) total covered area on the surface. Data were analyzed by analysis of variance and post hoc Tukey test. The sequence of processing of SEM micrographs in relation to cell counts and the covered surfaces is illustrated in Fig 2.

Analysis of Chemical Composition

Energy dispersive x-ray analysis (EDX) was performed under SEM (TESCAN). One sample from each experimental group was selected randomly and attached to an aluminum stub (Agar Scientific). The specimens were then viewed under the SEM, and EDX was carried out to determine the constituent elements of implant surfaces.

© 2014 BY QUINTESSENCE PUBLISHING CO, INC. PRINTING OF THIS DOCUMENT IS RESTRICTED TO PERSONAL USE ONLY.
NO PART MAY BE REPRODUCED OR TRANSMITTED IN ANY FORM WITHOUT WRITTEN PERMISSION FROM THE PUBLISHER.

RESULTS

Number and Area of Cell Attachment

The means ± standard deviations of the amount of P19 cell attachment for Biohorizons, Biohorizons collar, Astra, Astra collar, Biomet, Biomet collar, ITI, ITI collar, and zinc oxide–eugenol surfaces are presented in Table 1. The post hoc Tukey test demonstrated significant differences in P19 cell counts between all the modified and electropolished surfaces ($P < .05$). The highest P19 cell counts were shown on the OsseoSpeed-treated collars, followed by Laser-Lok surfaces, with no significant differences between these two surfaces ($P = .061$). P19 cell counts were significantly higher on the OsseoSpeed and Laser-Lok surfaces on the collars in comparison with OsseoSpeed and RBM treatments on the body surfaces ($P = .0001$ and $P = .032$, respectively). This value was not significantly different between SLActive and Nanotite surfaces both on the collar and body surfaces ($P = .963$ and $P = .201$, respectively). SLActive and Nanotite treatments on the body of implants showed higher cell counts in comparison with collar parts; however, the differences were not significant. The lowest value was shown on the Nanotite collars, which differed significantly from other test groups, but it was not different from Nanotite body surfaces ($P < .05$). In the negative control group (gutta-percha group), counting was impossible because of the large number of cells covering the surface and confluence; therefore, the authors did not consider this group for statistical analysis.

The extent of cell-covered surface area is presented (means ± standard deviations) in Table 1. The post hoc Tukey test revealed significantly greater surface areas on all the test surfaces compared to the control surfaces ($P < .05$). Comparison of the implant bodies and treated collar surfaces showed the largest cell-covered surface area on Laser-Lok surfaces, followed by OsseoSpeed collar surfaces, with no significant difference between these two ($P = 1.000$). The Laser-Lok and OsseoSpeed collar parts showed significant differences versus RBM and OsseoSpeed bodies ($P = .008$ and $P = .015$), while this difference was not seen between SLActive and Nanotite collar and body surfaces ($P = .589$ and $P = 1.000$). Unlike cell count values, the covered surface area on the SLActive collar region was larger than that on the SLActive implant body, with no significant difference ($P = .589$).

EDX Findings

EDX revealed titanium, aluminum, and vanadium elements on the Biohorizons and Biomet 3i implants; pure titanium was observed on the ITI and Astra Tech implants (Figs 3a to 3d).

Table 1 Means ± Standard Deviations of P19 Cell Counts and Cell-Covered Surface Areas

Surface	No. of cells	Surface area covered by cell (μm)
Biohorizons (RBM)	537.2 ± 92.7	3.98 ± 0.63
Biohorizons collar (Laser-Lok)	657 ± 45.11	5.75 ± 1.07
Astra body (OsseoSpeed)	448 ± 61.61	3.87 ± 0.49
Astra collar (OsseoSpeed)	767.6 ± 52.46	5.54 ± 1.46
Biomet 3i (Nanotite)	398.6 ± 31.02	2.65 ± 0.31
Biomet 3i collar (Nanotite)	307.40 ± 75.87	2.46 ± 0.49
ITI (SLActive)	497 ± 23.10	3.11 ± 0.11
ITI collar (SLActive)	457.60 ± 46.07	3.97 ± 0.32
Electropolished	19.4 ± 6.10	0.01 ± 0.00

DISCUSSION

Previous studies have shown that implant surfaces might be adsorbed in the body, resulting in systemic neurotoxicity.[5] In 2010, Wu et al[18] investigated the roles of particle size and the crystal structure of TiO_2 nanoparticles (NPs) in neurotoxicity and reported that microsized TiO_2 did not exhibit any toxic response. However, the NPs displayed dose-dependent neurotoxicity. Release of any TiO_2 remnants from the implant surface might have an influence on the electrical excitability of nerves via concentration of permanent ions and through affecting the gating process of ion channels.[19] On the other hand, Wennerberg and Albrektsson analyzed the ionic leakage of moderately roughened surfaces to detect biologic effects of such leakage and reported no dangerously higher levels of corrosion.[16] Wada et al demonstrated that nerve fibers in peri-implant bone in unloaded implant sites were poorly innervated, unlike the loaded implant sites, which were innervated, and it was proposed that these nerve endings play significant roles as mechanoreceptors.[10]

The results of the present study showed that P19 neural cells not only were capable of growing on all of these surfaces, although at different rates, but they also maintained their typical morphology. This is consistent with a 2009 study of Yuan et al,[20] which demonstrated the biocompatibility of implant surfaces to Schwann cells by increased levels of nerve growth factor and brain-derived neurotrophic factor.[20] The highest P19 cell counts were detected on the OsseoSpeed and Laser-Lok surfaces, with no significant differences between these two groups. Cell attachment to a surface

© 2014 BY QUINTESSENCE PUBLISHING CO, INC. PRINTING OF THIS DOCUMENT IS RESTRICTED TO PERSONAL USE ONLY.
NO PART MAY BE REPRODUCED OR TRANSMITTED IN ANY FORM WITHOUT WRITTEN PERMISSION FROM THE PUBLISHER.

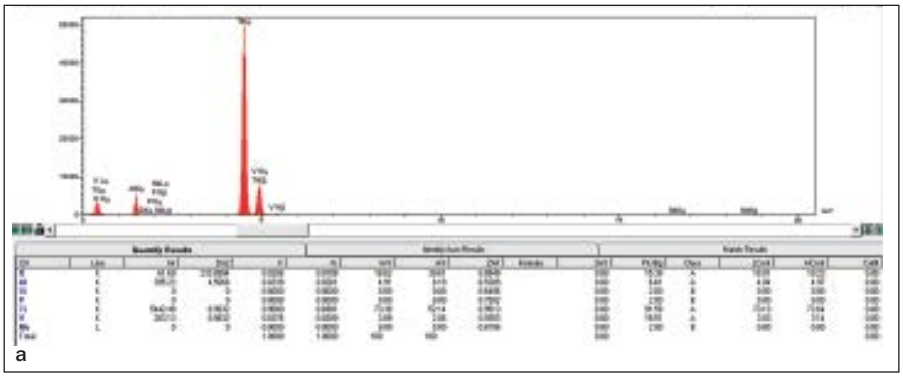

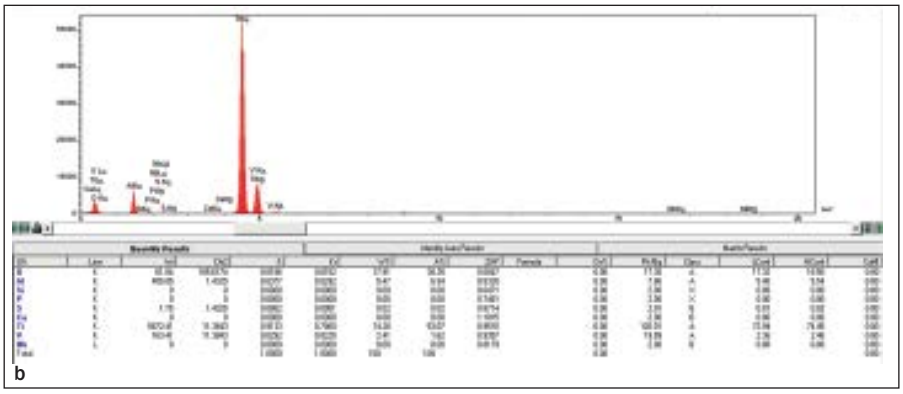

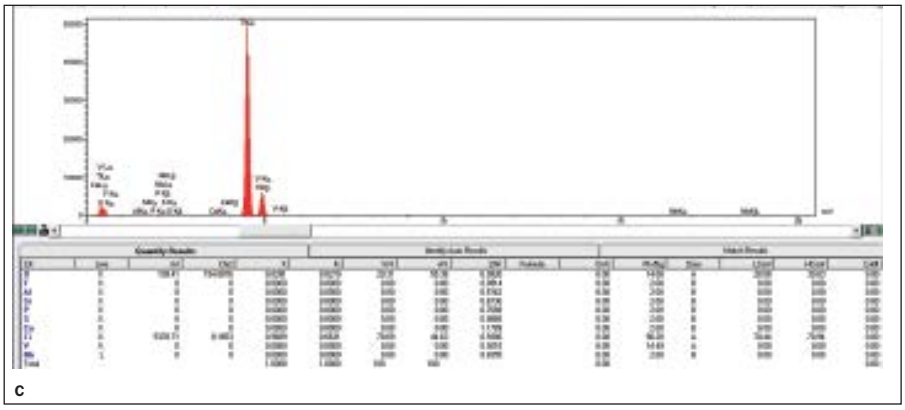

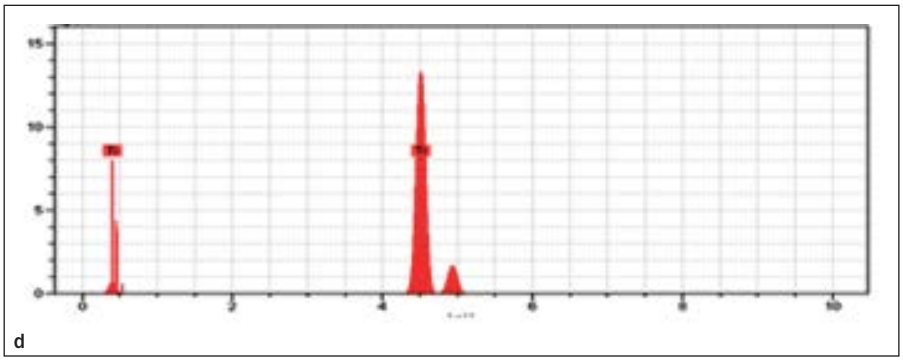

Figs 3a to 3d Energy dispersive spectroscopy. *Top to bottom*: Osseospeed (Astra), Nanotite (Biomet 3i), Laser-Lok and RBM (Biohorizons), SLActive (ITI).

© 2014 BY QUINTESSENCE PUBLISHING CO, INC. PRINTING OF THIS DOCUMENT IS RESTRICTED TO PERSONAL USE ONLY.
NO PART MAY BE REPRODUCED OR TRANSMITTED IN ANY FORM WITHOUT WRITTEN PERMISSION FROM THE PUBLISHER.



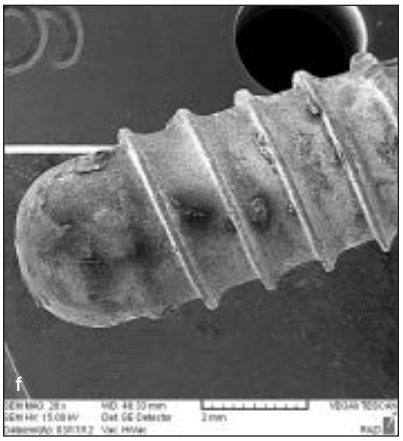

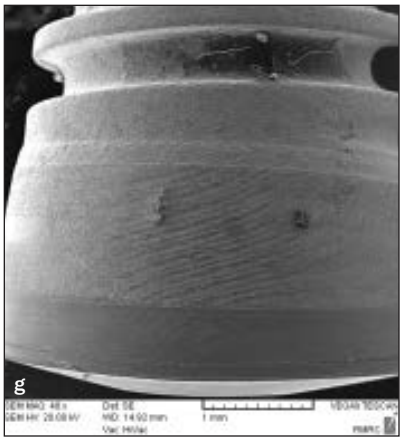

Fig 3e Resin injection gun from making replica of mold surface.

Figs 3f to 3i SEM images of (*f*) ITI implant surface, (*g*) Laser-Lok–treated collar part (note the microchannels formed after Laser-Lok treatment on the collar surface), (*h*) SLActive-treated implant body showing the length of distance between two threads, (*i*) SLActive-treated implant body showing the depth of a thread.

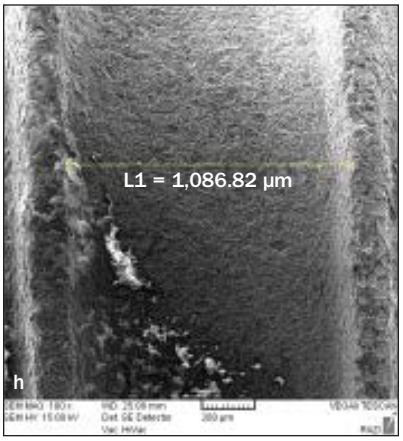

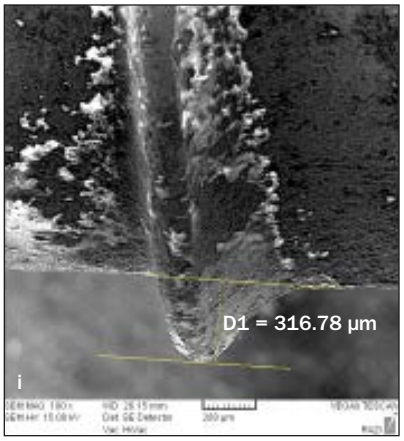

is affected by various surface characteristics, such as chemical composition and topography. Fan et al[21] examined the attachment and viability of cells from substantia nigra on silicon wafers with the same chemical composition and different surface roughness. These authors concluded that cell adhesion to etched rough surfaces with average surface roughness (Ra) in the range of 20 to 70 nm was significantly greater than that to untreated smooth surfaces; they also observed a network of neurons and axons on the etched surface, in contrast to isolated cells on the smooth surface, indicating different cell behaviors.[21] Laser-Lok surface treatment consists of 8- and 12-µm microchannels created by computer-controlled laser ablation, which optimally controls the orientation of attached cells. SEMs of implants retrieved from human volunteers showed the attachment of connective tissue fibers to the Laser-Lok microchannels, while on other implant surfaces, connective tissue fibers originated from the alveolar crest and moved parallel to the implant surface.[22,23] The higher count of P19 cells on the Laser-Lok surface might be a result of these microchannels, which control the adhesion and possibly the orientation of neural cells (Fig 3g).

The OsseoSpeed surface present on the implant body and collar parts contains 50- to 100-nm features made by TiO_2 blasting, followed by hydrofluoric acid etching, which leaves remnants of fluorine.[24,25] It has been demonstrated that the surface fluoride remnants promote precipitation of calcium and phosphorus ions by providing additional precipitation sites.[26] It would be suggested that the nanoscale roughness and modified chemical composition of the OsseoSpeed surface with the remaining fluorine groups might play an important role in the stronger P19 cell adhesion (Fig 1i). Interestingly, the values on the OsseoSpeed collar were higher than those seen on the implant body, irrespective of the same microdesign and chemical composition. Kim et al compared microgrooved orthodontic implants with nonmicrogrooved implants and found significantly higher bone-implant contact percentages for microgrooved implants. In addition, the microgrooved implants exhibited perpendicular or circular alignment of gingival connective tissue fibers to implant surface, in contrast to parallel fiber alignment in nonmicrogrooved implants.[7,8,27–29] Therefore, the significant difference between the OsseoSpeed implant body and collar could

© 2014 BY QUINTESSENCE PUBLISHING CO, INC. PRINTING OF THIS DOCUMENT IS RESTRICTED TO PERSONAL USE ONLY.
NO PART MAY BE REPRODUCED OR TRANSMITTED IN ANY FORM WITHOUT WRITTEN PERMISSION FROM THE PUBLISHER.

be attributed to microgrooves on the collar, which result in an increase in cell adhesion despite the same chemical composition and hydrophilicity (Fig 1h).

Cell counts and cell-covered area on the Nanotite collar showed higher values versus the electropolished collar of the ITI implant; however, these values were lower than those seen for other surfaces. Nanotite surfaces have nanoscale topography that is imparted via particulate sol-gel deposition using discrete crystalline deposition of calcium phosphate particles that are 20 to 100 nm. Based on SEM analysis, the Nanotite surface has a significantly lower surface roughness than the SLActive and OsseoSpeed surfaces and the densest structure.[9,10,30–32] On the other hand, one of the major drawbacks regarding calcium phosphate–coated implant surfaces is possible delamination of the coating caused by discrepancy in dissolution behavior between the amorphous and crystalline phases of coating.[5,11,24,26,30] This is expected to be more common with thin coatings because of the amorphous structure, which might hinder short- and long-term implant success.[24] Implant surface–tissue interaction is affected by such chemical and physical surface properties as ionic composition, hydrophilicity, and surface roughness. The aforementioned factors might be important in lower P19 cell counts on the Nanotite surfaces.

The SLActive surfaces, which are manufactured in a multiple-step process, including rinsing of the SLA (sandblasted, large-grit, acid-etched) surface under nitrogen protection to prevent exposure to air and storage in a sealed saline-containing tube. This manufacturing method can result in a decrease in contact angle and an increase in hydrophilicity, which is reported to improve the chemical and physical properties. In addition, the modification of the SLA surface to the SLActive surface can establish more oxygen and titanium and lower the carbon concentration, resulting in greater osteoblastic phenotype differentiation on this active surface. This can produce more alkaline phosphatase, along with more osteocalcin, prostaglandin E2, and transforming growth factor-β.[32] The results of the present study demonstrated that the measured values on SLActive implant bodies were not different from those of RBM, OsseoSpeed, and Nanotite surfaces of implant bodies. However, these values were lower than those measured on the Laser-Lok and OsseoSpeed collars. These differences might be attributed to the different chemical and physical environments of the SLActive surface.

The fewest cells and poorest cell coverage was observed on the electropolished implant collars. Zinger et al[28] investigated osteoblastlike cell adhesion to different implant surfaces. After 4 and 24 hours, the cell density was not different, but after 3 days, it was significantly lower on polished, electropolished, and SLA surfaces compared to anodized surfaces. They pointed out that different cell types demonstrated various responses to nanostructures. Epithelial, fibroblastic, and endothelial cells react in different manners to different groove depths compared to macrophagelike cells; this might be attributed to minor differences in chemical properties and surface charges, which might influence the various cell adhesion and spreading processes. In addition, these cells might be adhered via cell attachment to specific structural sites, eg, sharp reliefs.[28] Lim et al[17] found a positive relationship (decrease in wettability) between surface roughness and contact angle for angles greater than 45 degrees and a negative association (increase in wettability) for angles less than 45 degrees (Figs 3h and 3i).[17]

The results of cell counts and cell-covered surface area in different groups were similar except for minor differences, which might be attributed to the viability of P19 cells on different implant surfaces. Wu et al[18] evaluated the roles of particle size and crystal structure of TiO_2 NPs in neurotoxicity and reported that micro-sized TiO_2 did not display any toxic response; however, the NPs showed dose-dependent neurotoxicity. In the present study, two nanotopographic surfaces (OsseoSpeed and Nanotite) and three microtopographic surfaces (RBM, SLActive, and Laser-Lok) were evaluated; no significant differences were observed between them. This might be explained by the fact that the previous studies investigated free NPs (TiO_2 NPs), whereas the TiO_2 in dental implants is firmly attached to the implant body. Wennerberg and Albrektsson analyzed the ionic leakage of moderately roughened surfaces and reported no dangerously elevated levels of corrosion.[16] Fortunately, neurotoxicity in TiO_2 NPs is dose-dependent, and Lai et al[5] reported that none of the microparticles and NPs (TiO_2) are toxic at concentrations weaker than 1 μg/mL.

Previous investigators have discussed the toxic potential of titanium alloys resulting from metallic ion release, which is considered to be toxic.[31] Among alloys tested, vanadium-containing types have been shown to be cytotoxic for macrophages and fibroblasts, which can stimulate local and systemic reactions. It appears that the release of ions takes place after ion exchange occurring between the tissue fluid and implant surface, which is influenced by electrochemical and mechanical properties of the surface oxide layer.[31] The EDX micrograph of samples showed that Biohorizons and Biomet 3i implants, made of titanium alloys, demonstrated different reactions to P19 cells. Thus, the differences in cell attachment are probably unrelated to the toxic effect of titanium implants.

Improvement in the understanding of neurophysiologic integration of dental implants is not only the basis for advances in osseoperception, leading to better

© 2014 BY QUINTESSENCE PUBLISHING CO, INC. PRINTING OF THIS DOCUMENT IS RESTRICTED TO PERSONAL USE ONLY.
NO PART MAY BE REPRODUCED OR TRANSMITTED IN ANY FORM WITHOUT WRITTEN PERMISSION FROM THE PUBLISHER.

perception of external stimuli and avoidance of excessive forces. It is also required to modify implant surfaces to reduce neurotoxicity, especially in cases of impingement of neurovascular channels by dental implants.

CLINICAL IMPLICATIONS AND FUTURE SCOPE

Within the limitations of this experimental study, the following conclusions were drawn:

1. All five types of dental implant surfaces were able to promote P19 cell line growth on collar and body parts, demonstrating neurocompatibility of the tested surfaces.
2. The Laser-Lok and OsseoSpeed surface treatments on implant collars showed greater compatibility with neural P19 cells than the other surface treatments. Cell counts and cell-covered surface areas showed higher P19 counts on the collars of these implants.
3. The electropolished and Nanotite surfaces exhibited the lowest cell counts and surface coverage values.
4. Significant differences in cell counts and cell-covered areas between the treated collar and body parts of implants were noticed only for the Biohorizons and Astra Tech implant systems.

The authors suggest further clinical studies on the effects of different implant surfaces on osseoperception and the neurophysiologic properties of implant surfaces.

ACKNOWLEDGMENTS

This publication was based on a thesis presented to the Faculty of Periodontics at Azad University of Tehran, in partial fulfillment of the requirements for a Master of Science in Periodontics. The authors are indebted to Dr Amir Nazari for the provision of laboratory facilities in the Department of Dental Materials at the University of Tokyo. Also, special thanks are due to Professors Jack L. Ferracane, the late Kamal Asgar, and Dr Maryam Elyasi for all of their contributions to this research. The authors extend their special thanks to Mr Nasser Valaie for his invaluable help with statistics and data analyses.

The authors affirm that they have no financial affiliations or involvements with any commercial organization with direct financial interest in the subject or materials discussed in this manuscript and deny any conflicts of interest related to this study.

REFERENCES

1. Lang NP, Jepsen S. Implant surfaces and design (Working Group 4). Clin Oral Implants Res 2009;20:228–231.
2. Rehn B, Seiler F, Rehn S, Bruch J, Maier M. Investigations on the inflammatory and genotoxic lung effects of two types of titanium dioxide: Untreated and surface treated. Toxicol Appl Pharmacol 2003;189:84–95.
3. Warheit DB, Webb TR, Reed KL, Frerichs S, Sayes CM. Pulmonary toxicity study in rats with three forms of ultrafine-TiO_2 particles: Differential responses related to surface properties. Toxicology 2007;230:90–104.
4. Monteiller C, Tran L, MacNee W, et al. The pro-inflammatory effects of low-toxicity low-solubility particles, nanoparticles and fine particles, on epithelial cells in vitro: The role of surface area. Occup Environ Med 2007;64:609–615.
5. Lai JCK, Lai MB, Jandhyam S, et al. Exposure to titanium dioxide and other metallic oxide nanoparticles induces cytotoxicity on human neural cells and fibroblasts. Int J Nanomed 2008;3:533–545.
6. Wennerberg A, Albrektsson T, Andersson B, Krol J. A histomorphometric study of screw-shaped and removal torque titanium implants with three different surface topographies. Clin Oral Implants Res 1995;6:24–30.
7. Rasmusson L, Roos J, Bystedt H. A 10-year follow-up study of titanium dioxide–blasted implants. Clin Implant Dent Relat Res 2005;7:36–42.
8. Wang Y, Kojo T, Ando H, et al. Nerve regeneration after implantation in peri-implant area. A histological study on different implant materials in dogs. Osseoperception 1998;3:3–11.
9. Ysander M, Brånemark R, Olmarker K, Myers RR. Intramedullary osseointegration: Development of a rodent model and study of histology and neuropeptide changes around titanium implants. J Rehabil Res Dev 2001;38:183–190.
10. Wada S, Kojo T, Wang YH, et al. Effect of loading on the development of nerve fibers around oral implants in the dog mandible. Clin Oral Implants Res 2001;12:219–224.
11. Asrari M, Lobner D. In vitro neurotoxic evaluation of root-end–filling materials. J Endod 2003;29:743–746.
12. Mattson MP, Barger SW, Begley JG, Mark RJ. Calcium, free radicals, and excitotoxic neuronal death in primary cell culture. Methods Cell Biol 1995;46:187–216.
13. Mofid MM, Thompson RC, Pardo CA, Manson PN, Craig A, Kolk V. Biocompatibility of fixation materials in the brain. Plast Reconstr Surg 1997;100:14–20.
14. Saghiri MA, Asgar K, Daliri M, et al. Morphological behavior and attachment of p19 neural cells to root-end filling materials. Scanning 2010;32:369–374.
15. Khorasani MT, Mirzadeh H, Talebi A, Irani S, Daliri M. Tubular scaffold design of poly (L-lactic acid) for nerve tissue engineering: Preparation, characterization, and in vitro assay. Iran Polymer J 2009;18: 297–306.
16. Wennerberg A, Albrektsson T. On implant surfaces: A review of current knowledge and opinions. Int J Oral Maxillofac Implants 2010;25:63–74.
17. Lim YJ, Oshida Y, Andres CJ, Barco MT. Surface characterizations of variously treated titanium materials. Int J Oral Maxillofac Implants 2001;16:333–342.
18. Wu J, Sun J, Xue Y. Involvement of JNK and P53 activation in G2/M cell cycle arrest and apoptosis induced by titanium dioxide nanoparticles in neuron cells. Toxicol Lett 2010;199:269–276.
19. Onur MA, Taş Z, Gürpınar A, Şahin S, Çehreli MC. Morphologic, functional and behavioral effects of titanium dioxide exposure on nerves. Clin Oral Implants Res 2004;15:513–519.
20. Yuan Q, Liao D, Yang X, et al. Effect of implant surface microtopography on proliferation, neurotrophin secretion, and gene expression of Schwann cells. J Biomed Mater Res A Part A 2010;93:381–388.
21. Fan Y, Cui F, Chen L, Zhai Y, Xu Q, Lee I. Adhesion of neural cells on silicon wafer with nano-topographic surface. Appl Surf Sci 2002; 187:313–318.

© 2014 BY QUINTESSENCE PUBLISHING CO, INC. PRINTING OF THIS DOCUMENT IS RESTRICTED TO PERSONAL USE ONLY.
NO PART MAY BE REPRODUCED OR TRANSMITTED IN ANY FORM WITHOUT WRITTEN PERMISSION FROM THE PUBLISHER.

22. Nevins M, Nevins ML, Camelo M, Boyesen JL, Kim DM. Human histologic evidence of a connective tissue attachment to a dental implant. Int J Periodontics Restorative Dent 2008;28:111–121.
23. Boyesen JL, Kim DM. Human histologic evidence of a connective tissue attachment to a dental implant. Restorative Dent 2008;28:111–121.
24. Junker R, Dimakis A, Thoneick M, Jansen JA. Effects of implant surface coatings and composition on bone integration: A systematic review. Clin Oral Implants Res 2009;20:185–206.
25. Cooper LF, Zhou Y, Takebe J, et al. Fluoride modification effects on osteoblast behavior and bone formation at TiO_2 grit-blasted cp titanium endosseous implants. Biomaterials 2006;27:926–936.
26. Jarmar T, Palmquist A, Brånemark R, Hermansson L, Engqvist H, Thomsen P. Characterization of the surface properties of commercially available dental implants using scanning electron microscopy, focused ion beam, and high-resolution transmission electron microscopy. Clin Implant Dent Relat Res 2008;10:11–22.
27. Kim TW, Baek SH, Kim JW, Chang YI. Effects of microgrooves on the success rate and soft tissue adaptation of orthodontic miniscrews. Angle Orthod 2008;78:1057–1064.
28. Zinger O, Anselme K, Denzer A, et al. Time-dependent morphology and adhesion of osteoblastic cells on titanium model surfaces featuring scale-resolved topography. Biomaterials 2004;25:2695–2711.
29. Ravichandran R. Biomimetic Surface Modification of Dental Implant for Enhanced Osseointegration [master's thesis]. Singapore: National University of Singapore, 2009.
30. Svanborg LM, Andersson M, Wennerberg A. Surface characterization of commercial oral implants on the nanometer level. J Biomed Mater Res B Appl Biomater 2010;92:462–469.
31. Assis S, Costa I. Electrochemical evaluation of Ti-13Nb-13Zr, Ti-6Al-4V, and Ti-6Al-7Nb alloys for biomedical application by long-term immersion tests. Mater Corros 2007;58:329–333.
32. Schwartz Z, Olivares-Navarrete R, Wieland M, Cochran DL, Boyan BD. Mechanisms regulating increased production of osteoprotegerin by osteoblasts cultured on microstructured titanium surfaces. Biomaterials 2009;30:3390–3396.

© 2014 BY QUINTESSENCE PUBLISHING CO, INC. PRINTING OF THIS DOCUMENT IS RESTRICTED TO PERSONAL USE ONLY.
NO PART MAY BE REPRODUCED OR TRANSMITTED IN ANY FORM WITHOUT WRITTEN PERMISSION FROM THE PUBLISHER.